Journal of
Vibration and Control

Fast-slow dynamic behaviors of a hydraulic generating system with multi-timescales

Journal:	*Journal of Vibration and Control*
Manuscript ID	JVC-18-0827.R1
Manuscript Type:	Original Manuscript
Date Submitted by the Author:	05-Mar-2019
Complete List of Authors:	Zhang, Jingjing; Northwest A&F University, Institute of Water Resources and Hydropower Research Chen , Diyi; Northwest A&F University, Electrical Department of College of Water Resources and Architectural Engineering, Zhang, Hao; Northwest Agriculture and Forestry University, Institute of Water Resources and Hydropower Research Xu, Beibei; Northwest A&F University, Institute of Water Resources and Hydropower Research Li, Huanhuan; Northwest A&F University, Institute of Water Resources and Hydropower Research Aggidis, George A.; Lancaster University, Faculty of Science & Technology, Engineering Department Engineering Building, Gillow Avenue, Office C08, Lancaster, LA1 4YW Chatterton, Steven; Politecnico di Milano, Mechanical Engineering
Keywords:	hydraulic generating system, multi-timescales, periodic excitation, fast-slow dynamic, nonlinear behaviors
Please select up to 5 subject areas that best reflect the content of your manuscript:	Fundamental dynamics,Modeling, Non-linear dynamics , Identification, Random vibrations, Analytical methods
Abstract:	Hydraulic generating systems, are widely modeling in the literature for investigating their stability properties by means of transfer functions representing the dynamic behavior of the reservoir, penstock, surge tank, turbine sand the generator. Traditionally, in these models the electrical load is assumed constant to simplify the modeling process. This assumption can hide interesting dynamic behavior caused by fluctuation of the load as actually occurred. Hence, in this study, the electrical load characterized with periodic excitation is introduced into a hydraulic generating system and the responses of the system show a novel dynamic behavior called the fast-slow dynamic phenomenon. To reveal the nature of this phenomenon, the effect of the three parameters (i.e. differential adjustment coefficient, amplitude, and frequency) on the dynamic behaviors of the hydraulic generating system is investigated, and the corresponding change rules are presented. The results show that the intensity of the fast-slow dynamic behaviors varies with the change of each parameter, which provides reference for the quantification of the hydraulic generating system parameters. More importantly, these results

	not only present rich nonlinear phenomena induced by multi-timescales, but also provide some theoretical bases for maintaining the safe and stable operation of a hydropower station.

Fast-slow dynamic behaviors of a hydraulic generating system with multi-timescales

Jingjing Zhang[1], Diyi Chen[1,2*], Hao Zhang[1], Beibei Xu[1], Huanhuan Li[1], George A. Aggidis[3], Steven Chatterton[4]

[1]*Institute of Water Resources and Hydropower Research; Key Laboratory of Agricultural Soil and Water Engineering in Arid and Semiarid Areas, Ministry of Education, Northwest A&F University, Shaanxi Yangling 712100, P.R. China*

[2]*Australasian Joint Research Centre for Building Information Modelling, School of Built Environment, Curtin University, WA 6102, Australia*

[3]*Lancaster University, Faculty of Science & Technology, Engineering Department, The New Engineering Building, Gillow Avenue, Office C08, Lancaster, LA1 4YW*

[4]*Politecnico di Milano, Deprtment Mechanical Engineering, I-20156 Milan, Italy*

Corresponding author: Diyi Chen

Telephones: 086-181-6198-0277

E-mail: diyichen@nwsuaf.edu.cn

Abstract: Hydraulic generating systems, are widely modeling in the literature for investigating their stability properties by means of transfer functions representing the dynamic behavior of the reservoir, penstock, surge tank, turbine sand the generator. Traditionally, in these models the electrical load is assumed constant to simplify the modeling process. This assumption can hide interesting dynamic behavior caused by fluctuation of the load as actually occurred. Hence, in this study, the electrical load characterized with periodic excitation is introduced into a hydraulic generating system and the responses of the system show a novel dynamic behavior called the fast-slow dynamic phenomenon. To reveal the nature of this phenomenon, the effect of the three parameters (i.e. differential adjustment coefficient, amplitude, and frequency) on the dynamic behaviors of the hydraulic generating system is investigated, and the corresponding change rules are presented. The results show that the intensity of the fast-slow dynamic behaviors varies with the change of each parameter,

which provides reference for the quantification of the hydraulic generating system parameters. More importantly, these results not only present rich nonlinear phenomena induced by multi-timescales, but also provide some theoretical bases for maintaining the safe and stable operation of a hydropower station.

Keywords: hydraulic generating system; multi-timescales; periodic excitation; fast-slow dynamic; nonlinear behaviors

1 Introduction

Hydraulic generating system is a complex nonlinear system coupled by several subsystems, namely hydraulic system, mechanical system and electrical system (Pennacchi et al., 2012; Aggidis et al. 2014; Xu et al., 2016). The system involves multi-timescales in operation because of the different response rates of the subsystem, which leads to the occurrence of richer dynamic behaviors compared with the same scale, such as bursting oscillation. Such oscillation, known as the quiescent state (QS) and spiking state (SP), is characterized by a cluster of large amplitude oscillations that alternate with the line-like small amplitude oscillations, which may lead to some special forms of bursting phenomena (Bi et al., 2011; Izhikevich 2000; Zhang et al., 2013; Sakaguchi et al., 2016; Shin et al., 2017). This special phenomena has a great influence on the safe and stable operation of a hydropower station. Therefore, from the point of view of an engineer, it is a challenge to study the safe operation of a hydraulic generating system by the theory of multi-timescales.

Fast-slow dynamic analysis is the common method of studying multi-timescales coupling system and it is widely used in biology, physics, etc. (Teka et al., 2012; Bertram et al. 2017; Upadhyay et al., 2017). For example, in the biology field, Belykh et al. simulated the bursting and spiking dynamics of many biological cells and reveal the mechanism of different fast-slow dynamics (Belykh et al., 2000). Wang et al. used fast-slow decomposition method to understand the multi-timescale mechanisms underlying sigh generation (Wang et al., 2017). Jia et al. learnt that the burst of the synchronous behaviors manifests the same pattern as the square negative current-induced burst of the isolated single neuron with the fast-slow variable dissection method (Jia et al., 2018). Song et al. studied the bursting behavior based on the bifurcation mechanisms and found that time delay must be large enough for bursting behavior to occur in a delayed system (Song et al., 2016). In the physics field, Strani presented a general procedure to describe slow dynamics in parabolic-hyperbolic systems, under suitable assumptions on the terms appearing in the equations (Strani 2018). Rubin et al. employed techniques of separating the dynamics of fast and slow variables to guide model development and achieve desired qualitative and quantitative solution properties (Rubin et al., 2018). Han et al. presented a general method to analyze mixed-mode oscillations and externally excited systems with two low excitation frequencies (Han et al., 2015). Yu et al. analyzed the dynamics of the Van Der Pol-Duffing fast-slow oscillator controlled by the parametric delay feedback (Yu et al., 2018). Actually, such fast-slow dynamic behaviors exist not only in the above field but also in the hydraulic generating system. However, as for the hydraulic generating system, a number of researchers have paid attention to studying the dynamic behaviors on the same time scale (Nanda et al., 2015; Beran et al., 2013; Soundarrajan et al., 2011; Chen et al., 2013; Yi et al., 2018; Helseth et al., 2013; Riasi et al., 2017). A few published papers have been obtained with fast-slow dynamics method to study the system dynamic behaviors (Zhang et al., 2017; Zhang et al., 2018; Li et al., 2018). Therefore, it is essential to study the interesting scientific questions about fast-slow dynamic behaviors of the hydraulic generating system to reveal the complex nonlinear phenomenon under multi-timescales.

Motivated by the above discussions, this paper has three advantages which make the approach attractive comparing with the prior works. Firstly, from the perspective of an engineer, a hydraulic generating system model with periodic excitation is established considering the fluctuation of electrical load. Secondly, it is found that fast-slow dynamic phenomena occur simultaneously in several state parameters of a high-dimensional system for the first time, because of a slight change of a single variable (i.e. the differential adjustment coefficient, the frequency or the amplitude), and the fast-slow dynamic phenomena are shown in detail. For example, the fast-slow dynamic phenomena become strong with the increase of the differential adjustment coefficient and the frequency, while the opposite conclusions can be obtained with the increase of the amplitude. Finally, from the point of view of engineering, the stable operation rules of a hydraulic generating system are analyzed using fast-slow dynamic analysis, and the relative deviation of turbine speed is an observable parameter with the current technology.

The rest of this paper is organized as follows. In Section 2, the hydraulic generating system model considering multi-timescales is described. Section 3 shows the effect of the differential adjustment coefficient, the amplitude and the frequency on the fast-slow dynamic behaviors of the hydraulic generating system in detail. Finally, the brief conclusions close this paper in Section 4.

2 Hydraulic generating system model

From the point of view of engineering and nonlinear dynamics, a hydraulic generating system with an upstream surge tank is chosen to study the fast-slow dynamic behaviors. The structural diagram of the hydraulic generating system is shown in **Fig. 1**. It consist of a reservoir, a diversion tunnel, a surge tank, a penstock, a hydro-turbine-generator unit and a draft tube.

Fig. 1. Structural diagram of a hydraulic generating system with upstream surge tank.

The dynamic characteristic of generator and load is (Ling 2007)

$$T_{ab}\frac{dx}{dt}+e_n x=m_t-m_{g0} \tag{1}$$

Fig. 2. Diagram of the hydraulic-mechanical system with upstream surge tank.

According to **Fig. 2**, the state equation for the hydraulic-mechanical system is obtained as

$$\begin{cases} \dfrac{dq_1}{dt} = -\dfrac{h_{f1}}{T_{w1}} q_1 - \dfrac{h_2}{T_{w1}} \\ \dfrac{dh_2}{dt} = \dfrac{q_1}{T_j} - \dfrac{e_{qh}}{T_j}(h_2 + h_3) - \dfrac{e_{qy}}{T_j} y \\ \dfrac{dh_3}{dt} = -\dfrac{q_1}{T_j} + \dfrac{e_{qh}}{T_j} h_2 + \left(\dfrac{e_{qh}}{T_j} - \dfrac{1}{e_{qh} T_{w3}}\right) h_3 + \dfrac{e_{qy}}{T_j} y - \dfrac{e_{qy}}{e_{qh}} \dfrac{dy}{dt} \end{cases} \tag{2}$$

where $e_y = e_{ym}(h_3 + 1)$, $e_{qy} = e_{qym}\sqrt{h_3 + 1}$, $e_x = e_{xm}\sqrt{h_3 + 1}$, $e_{qx} = e_{qxm}$, $e_h = e_{hm}$, $e_{qh} = e_{qhm}/(x+1)$ (Shen 1998; Fang 2005).

The hydro-turbine torque is

$$m_t = e_h(h_2 + h_3) + e_y y \tag{3}$$

The dynamic characteristics of a hydraulic servo system can be got as

$$T_y \frac{dy}{dt} + y = u \tag{4}$$

From Eq. (1) to Eq. (4) the dynamic model of the hydraulic generating system can be written as

$$\begin{cases} \dfrac{dq_1}{dt} = -\dfrac{h_{f1}}{T_{w1}} q_1 - \dfrac{h_2}{T_{w1}} \\ \dfrac{dh_2}{dt} = \dfrac{q_1}{T_j} - \dfrac{e_{qhm}}{T_j(x+1)}(h_2 + h_3) - \dfrac{e_{qym}}{T_j} y\sqrt{h_3 + 1} \\ \dfrac{dh_3}{dt} = -\dfrac{q_1}{T_j} + \dfrac{e_{qhm}}{T_j(x+1)} h_2 + \left[\dfrac{e_{qhm}}{T_j(x+1)} - \dfrac{x+1}{e_{qhm} T_{w3}}\right] h_3 + \dfrac{e_{qym}}{T_j} y\sqrt{h_3 + 1} - \dfrac{e_{qym}}{e_{qhm} T_y}(x+1)\sqrt{h_3 + 1}\left[k_p(r - x) + k_i x_4 - k_d \dfrac{dx}{dt} - y\right] \\ \dfrac{dx}{dt} = \dfrac{1}{T_{ab}}\left[e_{hm}(h_2 + h_3) + e_{ym}(h_3 + 1)y - e_n x - m_{g0}\right] \\ \dfrac{dy}{dt} = \dfrac{1}{T_y}(u - y) \end{cases} \tag{5}$$

The hydraulic generating system is a typical complex system involving different time scales. More specially, the time scale of the hydraulic system is minute level, the time scale of the mechanical system is second level and the time scale of the electrical system is nanosecond level. Its dynamic characteristics are affected by hydraulic factors, mechanical factors, electrical factors, etc.. Although the electrical load is always changing with the system operation varying, it appears likely to be a periodical state (Rostamkolai et al., 1994; Mandal et al. 2007). Therefore, the periodic excitation is introduced in this paper to describe the change rule of the electrical load

$$m_{g0} = A\sin(wt), \tag{6}$$

where A and w are the amplitude and the frequency of the periodic excitation, respectively.

A common PID control method is used in this paper, therefore a novel hydraulic generating system introducing periodic excitation is obtained as

$$\begin{cases} \dfrac{dq_1}{dt} = -\dfrac{h_{f1}}{T_{w1}} q_1 - \dfrac{h_2}{T_{w1}} \\ \dfrac{dh_2}{dt} = \dfrac{q_1}{T_j} - \dfrac{e_{qhm}}{T_j(x+1)}(h_2+h_3) - \dfrac{e_{qym}}{T_j} y\sqrt{h_3+1} \\ \dfrac{dh_3}{dt} = -\dfrac{q_1}{T_j} + \dfrac{e_{qhm}}{T_j(x+1)} h_2 + [\dfrac{e_{qhm}}{T_j(x+1)} - \dfrac{x+1}{e_{qhm}T_{w3}}]h_3 + \dfrac{e_{qym}}{T_j} y\sqrt{h_3+1} - \dfrac{e_{qym}}{e_{qhm}T_y}(x+1)\sqrt{h_3+1}[k_p(r-x)+k_i x_4 - k_d\dfrac{dx}{dt} - y] \\ \dfrac{dx}{dt} = \dfrac{1}{T_{ab}}[e_{hm}(h_2+h_3)+e_{ym}(h_3+1)y - e_n x - A\sin(wt)] \\ \dfrac{dy}{dt} = \dfrac{1}{T_y}[k_p(r-x)+k_i x_4 - k_d\dfrac{dx}{dt} - y] \\ \dfrac{dx_4}{dt} = r - x \end{cases} . \qquad (7)$$

The nomenclatures in Eqs. (1-7) are presented in **Table 1**.

Table 1. Hydraulic generating system model parameters.

3 Numerical experiments

The relative deviation of the flow in headrace tunnel (q_1), the relative deviation for the base head of surge tank (h_2), the inlet head of hydro-turbine (h_3) and the relative deviation of turbine speed (x) are the key parameters for the stability of the hydraulic generating system with the changing of the differential adjustment coefficient (k_d), the amplitude (A) or the frequency (w) based on the repeated numerical experiments. In the following contents, we focus on the dynamic characteristics of q_1, h_2, h_3 and x with periodic excitation. Here, the values of the basic system parameters are shown in **Table 2** and the numerical experiment results are carried out as shown in **Figs. 3-5**.

Table 2. The values of the system parameters.

3.1 System responses as the differential adjustment coefficient (k_d) changes

In order to reveal k_d with periodic excitation, the numerical experiments are carried out in **Fig. 3** where A=0.005 and w=0.1. In addition, k_d=1.24 is chosen to analyze the changing rules in time waveforms and phase trajectory.

Fig. 3. Fast-slow dynamic responses of the hydraulic generating system for A=0.005, w=0.1.

From **Fig. 3**, there are rich fast-slow dynamic phenomena for q_1, h_2, h_3 and x, which are interesting phenomena because fast-slow dynamic behaviors occur simultaneously in four parameters of a high-dimensional complex system with only one parameter (i.e. k_d) varying. From **Fig. 3(a1)**, the bifurcation diagram shows a strip distribution with different density in the longitudinal direction. The sparse part is the jump of the spiking state and the dense part is the quiescent state in part 1, which is consistent with the phase trajectory and time waveform. The fluctuation range of q_1 is decreasing with the increasing of k_d and a jump occurs in the lateral direction, which means that fast-slow dynamic behaviors of the system are weakening. As k_d increases further, the bifurcation diagram tends to be a straight line in part 2, which corresponds to the peak values of the spiking state as shown in **Fig. 3(a2)**. The bifurcation diagram shows that the stability of the system tends to be stable with the increase of k_d. Therefore, the values of k_d in part 2 is a good choice from the engineering point of view. From **Fig. 3(a2)**, small oscillations exist between the crests and troughs, while they are sufficiently weak, and hard to be observed in engineering.

It is noteworthy that similar phenomena occur in **Fig. 3(b)** compared with **Fig. 3(a)**. That is to say that some similar conclusions can be obtained, which are omitted for the sake of brevity. Conversely, h_2 shows some different dynamic characteristics compared with those of q_1. In comparing **Fig. 3(a1)** and **Fig. 3(b1)**, the two bifurcation diagrams show the different point density especially in the dense part. More intensive points in **Fig. 3(b1)** shows that the fast-slow dynamic behaviors of h_2 in **Fig. 3(b1)** are more obvious under the same parameter values, which can be easily observed in **Fig. 3(b2)** and **Fig. 3(b3)**. From **Fig. 3(b2)**, the relative deviation for h_2 starts with spiking state as it passes through the first period. The spiking state then disappears, and evolves towards the quiescent state 1. Finally, the first period finishes and a new cycle begins. It is apparent that the fluctuation of each state is different from another, which means that the fast-slow dynamic behaviors are not periodic. In each period, large and small amplitudes of oscillations coupling can consist of the fast-slow dynamic behaviors with multi-timescales.

Fig. 3(c1) shows similar dynamic behaviors compared with **Fig. 3(a1)** and **Fig. 3(b1)**. More specially, the fluctuation of h_3 gradually decreases, and fast-slow dynamic behaviors only occur in part 1. The characteristic of one period begins in spiking state and ends in quiescent state. Meanwhile, three different states also exist in **Fig. 3(c2)**. Compared with **Fig. 3(a2)** and **Fig. 3(b2)**, the fast-slow dynamic behaviors in **Fig. 3(c2)** are more obvious. There are also some specific phenomena. More specifically, there are some points above the straight line of part 2. The reason is that the oscillation amplitude of quiescent state is greater than that of the spiking state in **Fig. 3(c2)**.

For x, the bifurcation diagram, time waveform and phase trajectory are illustrated in **Fig. 3(d)**. From **Fig. 3(d1)**, the fluctuation of x gradually decreases and finally converges into two straight lines with the increase of k_d, which differ in **Figs. 3(a1)-3(c1)**. The reason discovered from **Fig. 3(d2)** is that the quiescent states occur at the crests in **Fig. 3(d2)**, while the quiescent states exist between the crests and the troughs in **Figs. 3(a2)-(c2)**. In addition, the amplitude of the quiescent state is larger than that of the spiking state.

From the above analysis, all the phenomena show that the fast-slow dynamic behaviors become weak as k_d increases. From the point of view of engineering practice, the fast-slow dynamic phenomena are harmful to the stability of the hydraulic generating system. To avoid the fast-slow dynamic behaviors, the values of k_d should be selected in the range of part 2. Meanwhile, h_3 in **Fig. 3(c)** and x in **Fig. 3(d)** oscillate vigorously compared with q_1 in **Fig. 3(a)** and h_2 in **Fig. 3(b)**. Among the four parameters, x is an observable parameter. Therefore, we can observe the value of x to judge the safety and stability of the hydraulic generating system.

3.2 System responses as the frequency (w) changes

The frequency (w) and the amplitude (A) are core parameters of periodic excitation. In order to reveal the effects of periodic excitation intensity on the system, firstly, w is extracted in this work to study the fast-slow dynamic behaviors of the presented hydraulic generating system in depth under periodic excitation. For the two parameters, A and k_d are cited as A=0.005 and k_d=1.3 in this subsection, respectively. To study the dynamical characteristics, w=0.1 in time waveforms and phase trajectory. The corresponding results are shown in **Fig. 4**.

Fig. 4. Fast-slow dynamic responses of the hydraulic generating system for A=0.005, k_d=1.3.

Fig. 4(a) displays the fast-slow dynamic responses of the hydraulic generating system for A=0.005, k_d=1.3. Mutation phenomena exist in **Fig. 4(a1)** because of the fast-slow dynamic behaviors as shown in **Figs. 4(a2)-4(a3)**. In **Fig. 4(a1)**, the sparse part and the dense part are the spiking state and the quiescent state in part 1, respectively. The values in part 2 equal the peak values of the large periodic oscillations (i.e. spiking state) in **Fig. 4(a2)**. The fluctuation range of q_1 is decreasing with the increase of w until it tends to be almost unchanged. This means that the fast-slow dynamic behavior becomes weak gradually until it disappears by increasing w. In other words, only certain frequency of an oscillation may suffice to achieve fast-slow dynamic behaviors, which is harmful to the stability of the hydraulic generating system. Therefore, the values of w in part 1 should be avoided in order to improve the stability of the system. From **Figs. 4(a2)-4(a3)**, the fast-slow dynamic behaviors of q_1 in **Fig. 3(a)** is so weak that it is difficult to observe.

The evolution rules of the fast-slow dynamic behaviors of the system can be obvious revealed in **Fig. 4(b1)**. More specifically, the bifurcation diagram in **Fig. 4(b1)** can also be divided into two parts. Part 1 demonstrates the fast-slow dynamic behaviors of the system, while the phenomenon disappears in part 2. This phenomenon indicates that the stability of the system improve as w increases. The values of part 2 are equal to the peak values of the spiking state in **Fig. 4(b2)**. **Figs. 4(b2)** and **Fig. 4(b3)** show that the fast-slow dynamic behaviors are characterized by a cluster of large amplitude oscillations that alternated with the line-like small amplitude oscillations. The fast-slow dynamic behaviors of h_2 are stronger than those of q_1. Therefore the relative deviation for h_2 is more sensitive to w. In addition, the quiescent state occurs in the latter part of a cycle, and then goes to another cycle. The oscillation fluctuation and duration time of each cycle is differs from each other, i.e., it shows non-periodic.

Similar change rules can be obtained in **Fig 4(c)** compared with **Figs. 4(a)-(b)** because of the similar dynamic behaviors. However, a difference also exists with each other. More sharp and obvious oscillations can be observed in **Fig 4(c)**. Some amplitudes of the spiking state are smaller than those of the quiescent state. It is consistent with the phenomenon that there are several points above the straight line in part 2 as shown in **Fig. 4(c1)**.

As for **Fig 4(d1)**, complex fast-slow dynamic behaviors arise in part 1. The fluctuation range of x shows similar tendency compared with that of **Figs. 4(a1)-(c1)**, i.e., the fluctuation range is decreasing and jump phenomenon exists in **Fig. 4(d1)**. The values of part 2 are consistent with the peak values of the spiking state in **Fig. 4(d2)**. The oscillation pattern of the relative deviation of turbine speed (x) in **Fig. 4(d)** is different with that of **Figs. 4(a)-(c)**. More specifically, the oscillation maintains spiking state at the beginning before the crest. At the crest, it exits the spiking state and enters the quiescent state. Then, the quiescent state disappears and evolves towards the spiking state again. Finally, a complete cycle of the fast-slow dynamic behaviors is completed and a new oscillation cycle commences.

All the above phenomena in **Figs. 4(a)-(d)** mean that only certain frequencies can lead to the fast-slow dynamic behaviors to occur. The fluctuation range lessens with the increase of w. Although the fast-slow dynamic behaviors exist in every variable, the intensity is differs in each other. The intensity of h_3 and x is stronger than that of q_1 and the relative deviation for h_2. Meanwhile, the values of w in part 2 can improve the stability of the system.

3.3 System responses as the amplitude (A) changes

In this subsection, A is chosen to investigate the fast-slow dynamic behaviors of the hydraulic generating system. Here, the values of k_d and w are 1.3 and 0.1, respectively. Note that A=0.0053 in the numerical experiments of time waveforms and phase trajectory.

Fig. 5. Fast-slow dynamic responses of the hydraulic generating system for k_d=1.3, w=0.1.

Bifurcation diagram, time waveform and phase trajectory in **Fig. 5(a)** show that fast-slow dynamic behaviors exist in the hydraulic generating system when A is assigned different values. **Fig. 5(a1)** is divided into two different parts, namely part 1 and part 2. The fluctuation range is almost unchanged in part 1, and the values correspond to the peak values in **Fig. 5(a2)**. The fluctuation range shows a significant change with the increase of A in part 2. As shown in part 2, the intensive section represents the quiescent state on the vertical axis, which is observable in **Fig. 5(a2)** and **Fig. 5(a3)**. On the horizontal axis, it is obvious that the fluctuation range of q_1 expand as A increase. The extensive range indicates that the fast-slow dynamic behaviors become stronger, which is harmful to the stability of the hydraulic generating system. In other words, the values of A should be in part 1 to improve the system reliability and stability. From **Fig. 5(a2)** and **Fig. 5(a3)**, the characteristic of the system is large periodic oscillations coupled with repeated small oscillations. There are weak fast-slow dynamic behaviors between the crests and the troughs. Therefore q_1 is not sensitive to A on the fast-slow dynamic behaviors.

Similar phenomenon also can be seen in **Fig. 5(b)**. Therefore, similar conclusions can be achieved, which are not illustrated in detail for the sake of brevity. In **Fig. 5(b1)**, it worth noting that the point density of h_2 is larger than that of q_1 in **Fig. 5(a1)**. The reason why this interesting phenomenon appears is that the fast-slow dynamic behaviors of q_1 are weaker than that of h_2. The general fluctuation trend of h_2 is in accordance with that of q_1, which enlarges with the increasing of A. The difference between q_1 and h_2 is the fluctuation intensity and duration time as shown in **Figs. 5(a2)-(a3)** and **Figs. 5(b2)-(b3)**. The quiescent states in **Fig. 5(a)** and **Fig. 5(b)** exist between the crests and the troughs. **Fig. 5(a)** and **Fig. 5(b)** also show that the cycle of the oscillation is the spiking state firstly and the quiescent state secondly.

Fig. 5(c) shows the interesting dynamic behaviors of the hydraulic generating system. As shown in **Fig. 5(c1)**, the fluctuation range is almost unchanged at the beginning and then increases suddenly as the amplitude (A) increases. There is an interesting phenomenon from part 1 to part 2 called jump. The straight line in part 1 not only indicates the system is in a stable state, but also presents the peak values of the spiking state. **Fig. 5(c2)** shows that the system is in the spiking state firstly, and then jumps into the quiescent state. The amplitudes of the quiescent state may exceed the peak values of the spiking state as shown in **Fig. 5(c2)**. Therefore, the values of some points are larger than those values in part 1 in **Fig. 5(c1)**.

From **Fig. 5(d1)**, the fluctuation range of x has a tendency to increase. More specially, the fluctuation range of x starts as straight lines in part 1 and then enlarges to an interval in part 2. It means that the system is in stable state in part 1, while the stability of the system deteriorates in part 2. It is further proved that the fast-slow phenomenon is unfavorable to the stability of the system. Therefore, the values of A in part 2 should be avoided from the point of view of reliability and stability. From **Figs. 5(d2)-(d3)**, the fast-slow dynamic behaviors are particularly obvious. Hence, x is observable or measurable under the existing technology. In other words, x is an important parameter to judge whether or not the hydraulic generating system shows fast-slow dynamic behaviors. In addition, the fast-slow dynamic behaviors only occur in crests in **Fig. 5(d2)**, i.e., the process of system evolution is spiking state, quiescent state and then spiking state.

From **Figs. 5(a)-(d)**, all the above phenomena suggest that the values of A have a great influence on the fast-slow dynamic characteristics of the hydraulic generating system. The fluctuation range of all variables is increasing with the increase of A. The system starts as the stable state, and then it goes into the unstable state with A varying. In addition, the fast-slow dynamic behaviors of h_3 and x are stronger than those of q_1 and the relative deviation for h_2. Meanwhile, the quiescent state of q_1, h_2 and h_3 occur between the crests and the troughs, while the quiescent state of x occurs at the crests.

4 Conclusions

Hydraulic generating system is a typical complex system with multi-timescales. In order to reveal the multi-timescales behaviors, the electrical load characterized with periodic excitation is introduced into the system. Based on this, the influences of differential adjustment coefficient, amplitude and frequency on the dynamic behaviors of the hydraulic generating system are investigated in detail by numerical experiments. First, the four parameters of the hydraulic generating system show different intensity fast-slow dynamic phenomena with the change of each variable. The oscillation intensity of the relative deviation for inlet head of hydro-turbine (h_3) and the relative deviation of turbine speed (x) is stronger than that of the relative deviation of the flow in headrace tunnel (q_1) and the relative deviation for the base head of surge tank (h_2). Second, the relative deviation of turbine speed (x) is an observable parameter to judge whether the system shows fast-slow dynamic behaviors based on the present technology. Third, the increase of amplitude (A) can enhance the fast-slow dynamic behaviors which are detrimental to the stability. Conversely, the fast-slow dynamic behaviors weaken as differential adjustment coefficient (k_d) or frequency (w) increase, which can improve the stability of the system.

Acknowledgements

This work was supported by the scientific research foundation of National Natural Science Foundation of China-Outstanding Youth Foundation (51622906).

Conflict of interest statement

The authors declare no conflict of interest in preparing this article.

References

Aggidis GA and Zidonis A (2014) Hydro turbine prototype testing and generation of performance curves: Fully automated approach. *Renew Energy* 71: 433-441.

Belykh VN, Belykh IV, Colding-Jørgensen M and Mosekilde E (2000) Homoclinic bifurcations leading to the emergence of bursting oscillations in cell models. *Eur Phys J E* 3(3): 205-219.

Beran V, Sedlacek M and Marsik F (2013) A new bladeless hydraulic turbine. *Appl Energy* 104: 978-983.

Bertram R and Rubin JE (2017) Multi-timescale systems and fast-slow analysis. *Math biosci* 287: 105-121.

Bi Q and Zhang Z (2011) Bursting phenomena as well as the bifurcation mechanism in controlled Lorenz oscillator with two time scales. *Phys Lett A* 375(8): 1183-1190.

Chen DY, Zhao WL, Ma XY and Wang J (2013) Control for a class of four-dimensional chaotic systems with random-varying parameters and noise disturbance. *Journal of Vibration and Control* 19(7): 1080-1086.

Fang HQ (2005) Nonlinear control strategy for hydraulic turbine generating unit and its industrial application research. Ph.D. thesis, Hohai university.

Han XJ, Bi QS, Ji P and Kurths J (2015) Fast-slow analysis for parametrically and externally excited systems with two slow rationally related excitation frequencies. *Phys Rev E* 92(1): 012911.

Helseth A, Gjelsvik A, Mo B and Linnet U (2013) A model for optimal scheduling of hydro thermal systems including pumped-storage and wind power. *IET Gener Transm Distrib* 7(12): 1426-1434.

Izhikevich EM (2000) Neural excitability, spiking and bursting. *Int J Bifurc Chaos* 10(6): 1171-1266.

Jia B, Wu YC, He D, Guo BH and Xue L (2018) Dynamics of transitions from anti-phase to multiple in-phase synchronizations in inhibitory coupled bursting neurons. *Nonlinear Dyn* 93(3): 1599-1618.

Li HH, Chen DY, Gao X, Wang XY, Han QS and Wu CZ (2018) Fast-slow dynamics of a hydropower generation system with multi-time scales. *Mech Syst Signal Pr* 110: 458-468.

Ling DJ (2007) Bifurcation and chaos of hydro-turbine governing system. Ph.D. thesis, Hohai university.

Mandal P, Senjyu T, Urasaki N, Funabashi T and Srivastava AK (2007) A Novel Approach to Forecast Electricity Price for PJM Using Neural Network and Similar Days Method. *IEEE T Power Syst* 22(4): 2058-2065.

Nanda J, Sreedhar M and Dasgypta A (2015) A new technique in hydro thermal interconnected automatic generation control system by using minority charge carrier inspired algorithm. *Int J Electr Power Energy Syst* 68: 259-268.

Pennacchi P, Chatterton S and Vania A (2012) Modeling of the dynamic response of a Francis turbine. *Mech Syst Signal Proc* 29: 107-119.

Riasi A and Tazraei P (2017) Numerical analysis of the hydraulic transient response in the presence of surge tanks and relief valves. *Renew Energ* 107: 138-146.

Rostamkolai N, Piwko RJ and Matusik AS (1994) Evaluation of the impact of a large cyclic load and the lilco power system using time simulation and frequency domain techniques. *IEEE T Power Syst* 9(3): 1411-1416.

Rubin JE, Krauskopf B and Osinga HM (2018) Natural extension of fast-slow decomposition for dynamical systems. *Physical Review E* 97(1): 012215.

Sakaguchi H and Okita T (2016) Cooperative dynamics in coupled systems of fast and slow phase oscillators. *Phys Rev E* 93(2): 022212.

Shen ZY (1998) Hydro-turbine governing system. 3rd ed. Beijing: Water Resources and Electric Power Press.

Shin J, Lee JH and Realff MJ (2017) Operational planning and optimal sizing of microgrid considering multi-scale wind uncertainty. *Appl Energ* 195: 616-633.

Song ZG and Xu J (2012) Codimension-two bursting analysis in the delayed neural system with external stimulations. *Nonlinear Dyn* 67(1): 309-328.

Soundarrajan A and Sumathi S (2011) Fuzzy-based intelligent controller for power generating systems. *Journal of Vibration and Control* 17(8): 1265-1278.

Strani M (2018) Semigroup estimates and fast-slow dynamics in parabolic-hyperbolic systems. *Adv Nonlinear Anal* 7(1): 117-138.

Teka W, Tabak J and Bertram R (2012) The relationship between two fast/slow analysis techniques for bursting oscillations. *Chaos* 22(4): 043117.

Upadhyay RK and Mondal A (2017) Synchronization of bursting neurons with a slowly varying d. c. current. *Chaos, Solitons and Fractals* 99: 195-208.

Wang YY and Rubin JE (2017) Timescales and Mechanisms of Sigh-Like Bursting and Spiking in Models of Rhythmic Respiratory Neurons. *J Math Neurosci* 7: UNSP 3.

Xu BB, Wang FF, Chen DY and Zhang H (2016) Hamiltonian modeling of multi-hydro-turbine governing systems with sharing common penstock and dynamic analyses under shock load. *Energy Convers Manage* 108: 478-487.

Yi YP, Zhang ZW , Chen DY, Zhou R, Patelli E and Tolo S (2018) State feedback predictive control for nonlinear hydro-turbine governing system. *Journal of Vibration and Control* 24(21): 4945-4959.

Yu Y, Zhang ZD and Bi QS (2018) Multistability and fast-slow analysis for van der Pol–Duffing oscillator with varying exponential delay feedback factor. *Appl Math Model* 57: 448-458.

Zhang H, Chen DY, Wu CZ and Wang XY (2018) Dynamics analysis of the fast-slow hydro-turbine governing system with different time-scale coupling. *Commun Nonlinear Sci Numer Simulat* 54:136-147.

Zhang H, Chen DY, Xu BB, Wu CZ and Wang XY (2017) The slow-fast dynamical behaviors of a hydro-turbine governing system under periodic excitations. *Nonlinear Dyn* 87(4): 2519-2528.

Zhang Z, Li Y and Bi Q (2013) Routes to bursting in a periodically driven oscillator. *Phys Lett A* 377(13): 975-980.

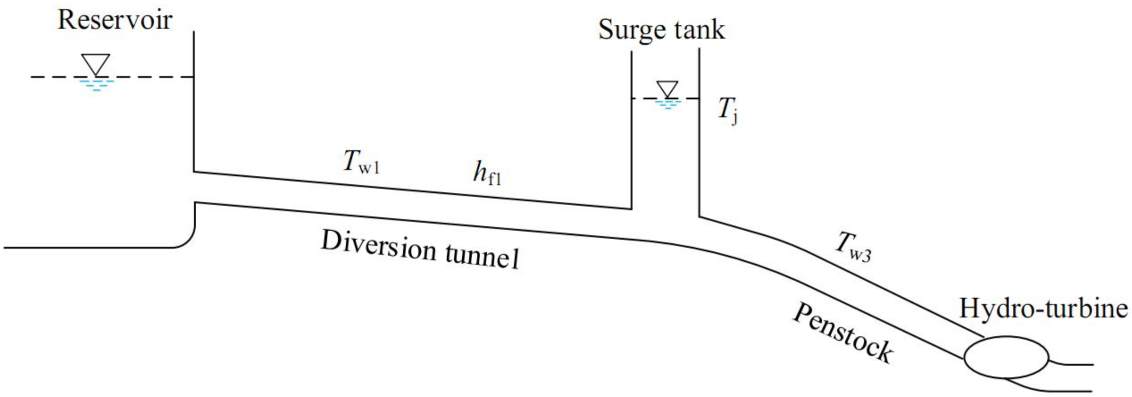

Fig. 1. Structural diagram of a hydraulic generating system with upstream surge tank.

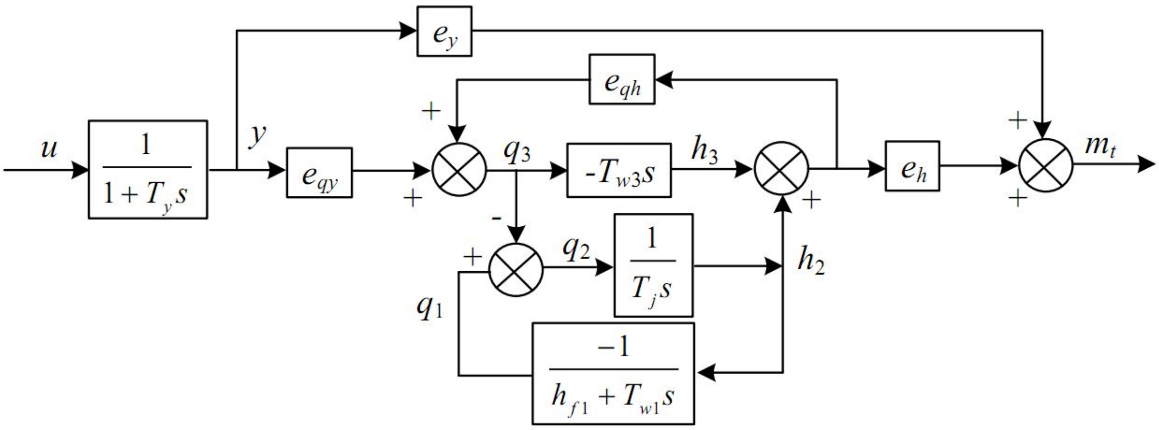

Fig. 2. Diagram of the hydraulic-mechanical system with upstream surge tank.

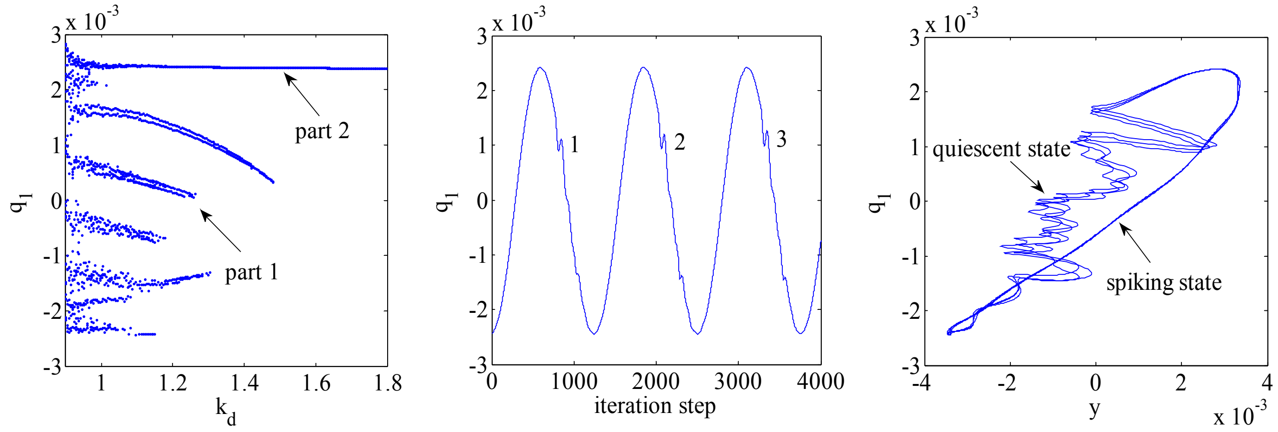

(a1) Bifurcation diagram of q_1-k_d. (a2) Time waveform of q_1. (a3) Phase trajectory of q_1-y.

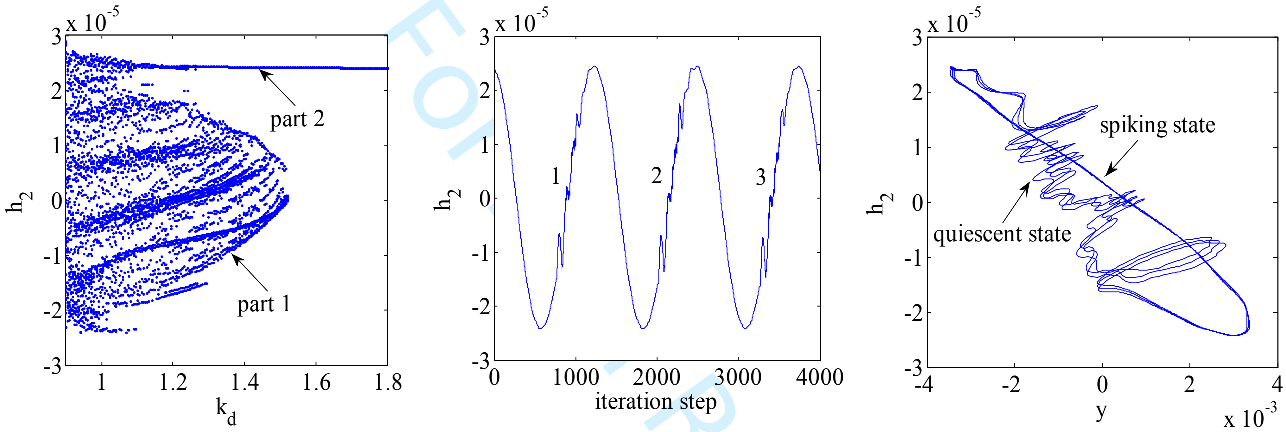

(b1) Bifurcation diagram of h_2-k_d. (b2) Time waveform of h_2. (b3) Phase trajectory of h_2-y.

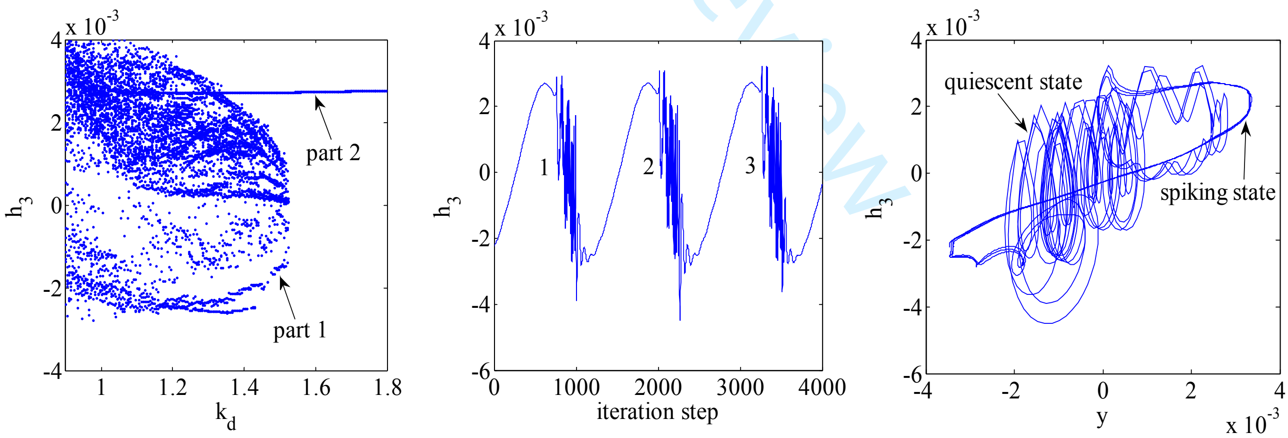

(c1) Bifurcation diagram of h_3-k_d. (c2) Time waveform of h_3. (c3) Phase trajectory of h_3-y.

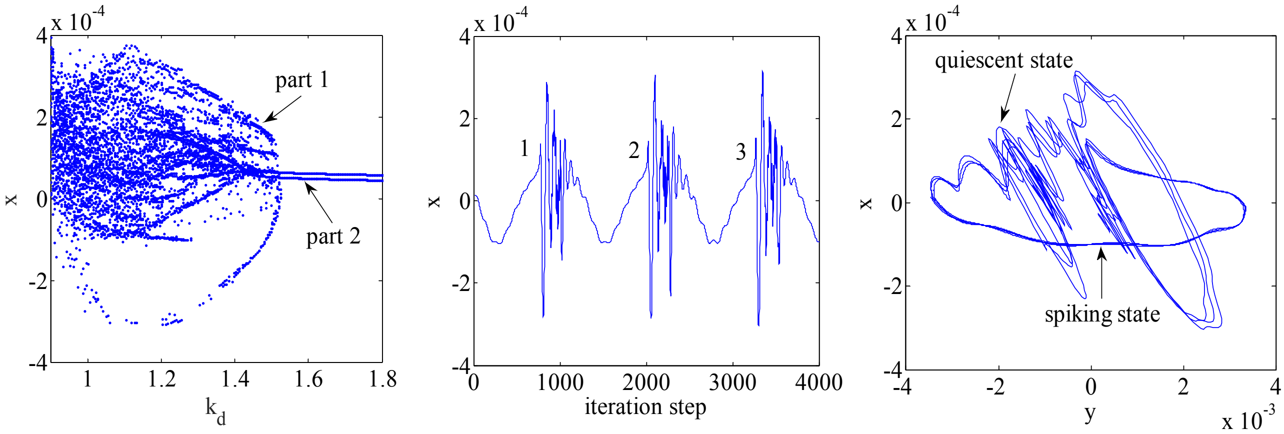

(d1) Bifurcation diagram of x-k_d. (d2) Time waveform of x. (d3) Phase trajectory of x-y.

Fig. 3. Fast-slow dynamic responses of the hydraulic generating system for A=0.005, w=0.1.

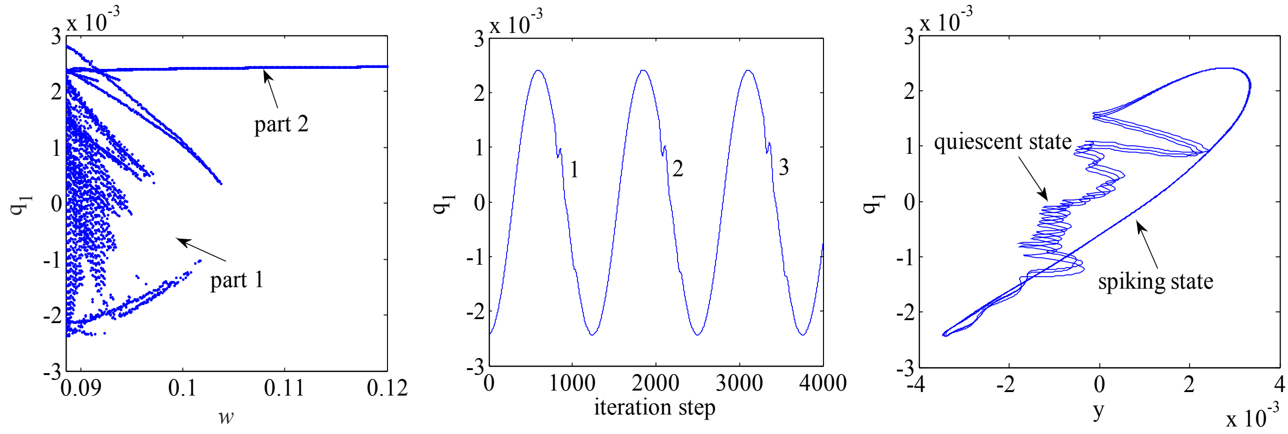

(a1) Bifurcation diagram of q_1-k_d. (a2) Time waveform of q_1. (a3) Phase trajectory of q_1-y.

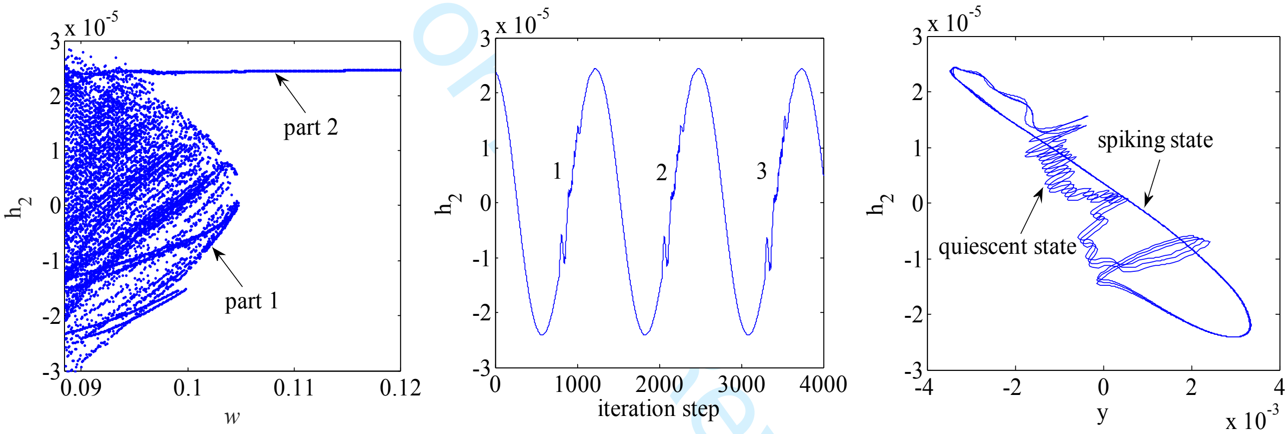

(b1) Bifurcation diagram of h_2-k_d. (b2) Time waveform of h_2. (b3) Phase trajectory of h_2-y.

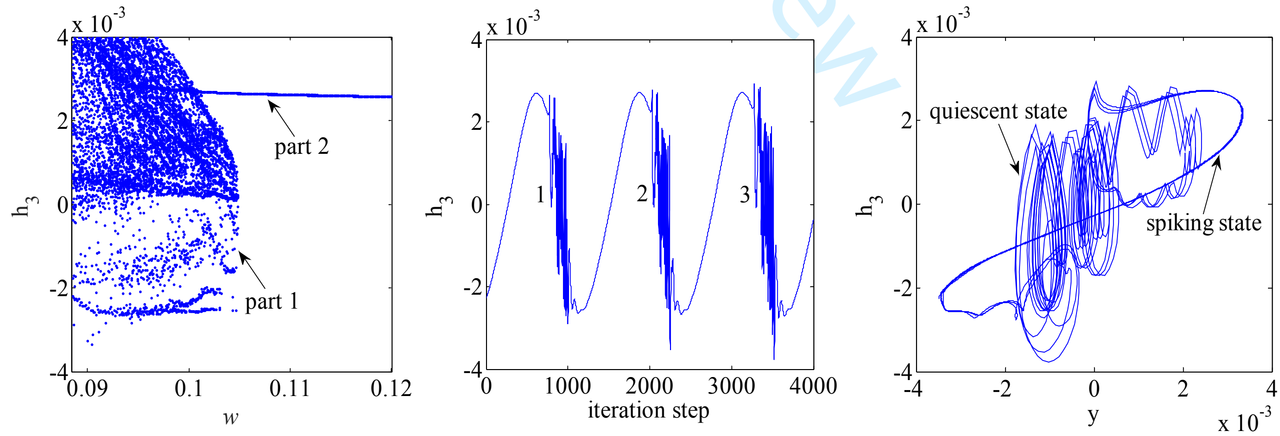

(c1) Bifurcation diagram of h_3-k_d. (c2) Time waveform of h_3. (c3) Phase trajectory of h_3-y.

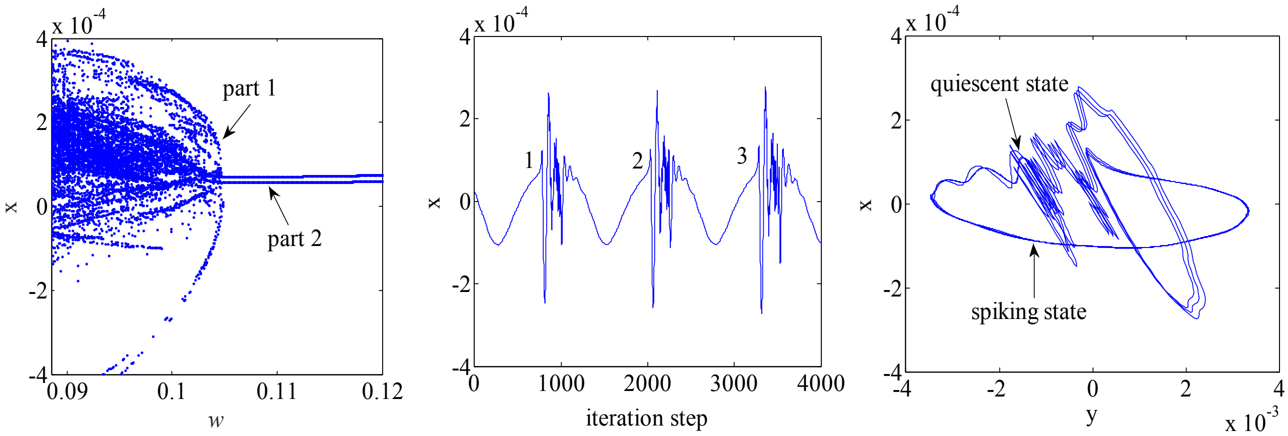

(d1) Bifurcation diagram of x-k_d. (d2) Time waveform of x. (d3) Phase trajectory of x-y.

Fig. 4. Fast-slow dynamic responses of the hydraulic generating system for A=0.005, k_d=1.3.

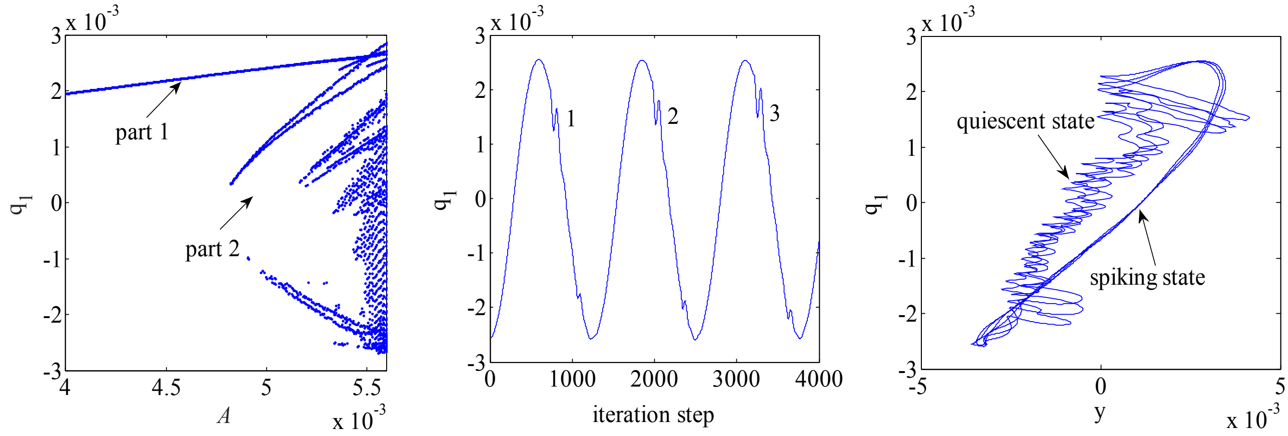

(a1) Bifurcation diagram of q_1-k_d. (a2) Time waveform of q_1. (a3) Phase trajectory of q_1-y.

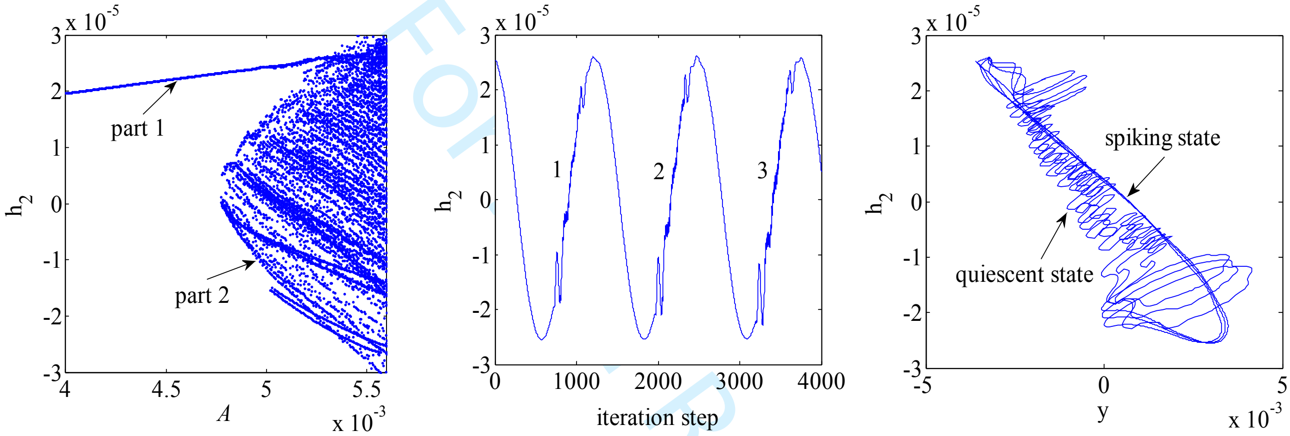

(b1) Bifurcation diagram of h_2-k_d. (b2) Time waveform of h_2. (b3) Phase trajectory of h_2-y.

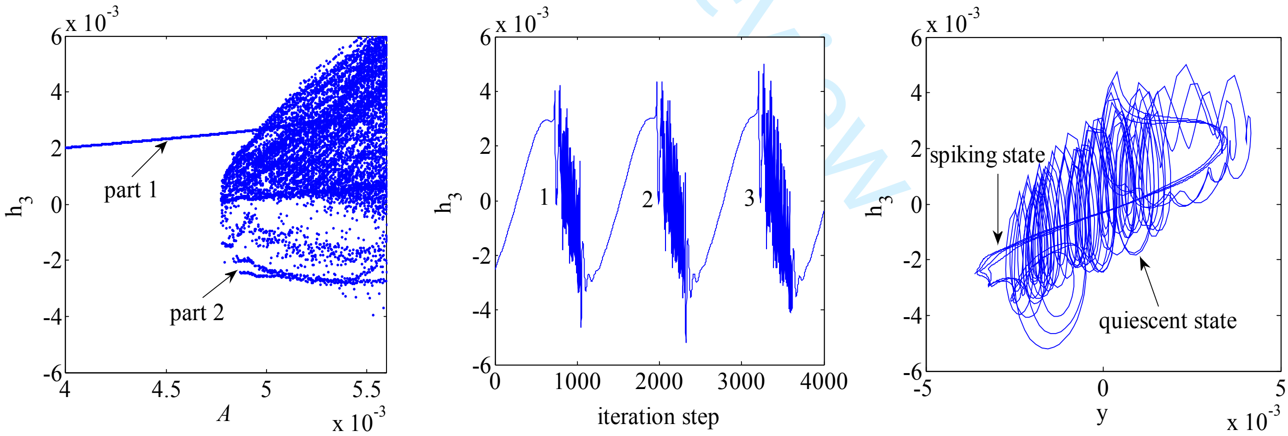

(c1) Bifurcation diagram of h_3-k_d. (c2) Time waveform of h_3. (c3) Phase trajectory of h_3-y.

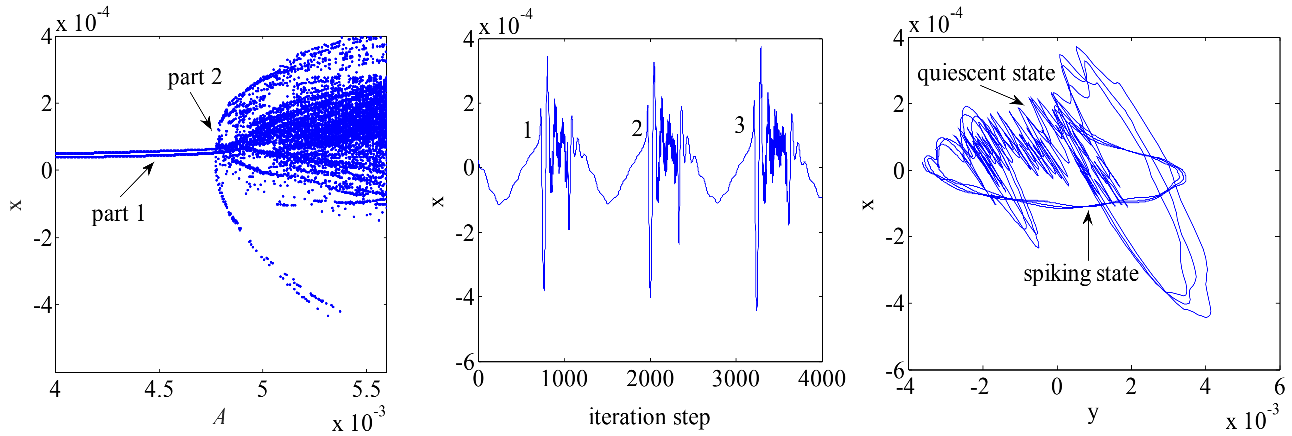

(d1) Bifurcation diagram of x-k_d. (d2) Time waveform of x. (d3) Phase trajectory of x-y.

Fig. 5. Fast-slow dynamic responses of the hydraulic generating system for k_d=1.3, w=0.1.

Table 1. Hydraulic generating system model parameters.

Symbols	Parameters
q_1	Relative deviation of the flow in diversion tunnel, p.u.
h_2	Relative deviation for the base head of surge tank, p.u.
h_3	Relative deviation for the inlet head of hydro-turbine, p.u.
x	Relative deviation of turbine speed, p.u.
y	Relative deviation of the guide vane opening, p.u.
x_4	Intermediate variable, p.u.
e_{qhm}, e_{qym}, e_{hm}, e_{ym}	Transfer coefficients, p.u.
T_{w1}	Flow inertia time constant of diversion tunnel, s
T_{w3}	Flow inertia time constant of penstock, s
T_{ab}	Hydro-turbine inertia time constant, s
T_{j}	Time constant of surge tank, s
h_{f1}	Frictional head loss of penstock, p.u.
T_{y}	Engager relay time constant, s
e_{n}	Synthetic self-regulation coefficient, p.u.
r	Reference input, p.u.
k_{p}	Proportional adjustment coefficient, p.u.
k_{i}	Integral adjustment coefficient, s^{-1}
k_{d}	Differential adjustment coefficient, s
A	Amplitude of the periodic excitation, p.u.
w	Frequency of the periodic excitation, p.u.

Table 2. The values of the system parameters.

Parameters	Values	Units	Parameters	Values	Units
e_{qhm}	0.55	p.u.	T_{j}	168	s
e_{qym}	0.6	p.u.	h_{f1}	0.01	p.u.
e_{hm}	1.3	p.u.	T_{y}	0.2	s
e_{ym}	1.2	p.u.	e_{n}	0.1	p.u.
T_{w1}	0.01	s	k_{p}	5	p.u.
T_{w3}	0.82	s	k_{i}	4.5	p.u.
T_{ab}	5.5	s			